RSC Advances

ROYAL SOCIETY OF CHEMISTRY

www.rsc.org/advances

Journal Name

RSCPublishing

ARTICLE

Fast and Highly Sensitive Humidity Sensors based on $NaNbO_3$ Nanofibers

Cite this: DOI: 10.1039/x0xx00000x

Youdong Zhang,[a] Xumin Pan,[a] Zhao Wang,[a,]* Yongming Hu,[a] Xiaoyuan Zhou,[b] Zhenglong Hu[c] and Haoshuang Gu[a]

Received 00th January 2012,
Accepted 00th January 2012

DOI: 10.1039/x0xx00000x

www.rsc.org/

A humidity sensor based on $NaNbO_3$ nanofiber networks was fabricated through the electrospinning process. The as-synthesized $NaNbO_3$ nanofibers with monoclinic perovskite structure are uniformly distributed and integrated by interdigital Pt/Ti electrodes on alumina substrates. The sensor exhibits fast and ultra-sensitive resistance type response to the variation of environmental humidity at room temperature. The sensor resistance is in logarithmic dependence on the relative humidity. The highest sensitivity is up to 10^5 for the humidity change from 20 to 80 %RH. Moreover, the response time for the humidification process is less than 3 s. The response time for dehumidification process is slower due to the slower desorption of water molecules. In addition, the sensor exhibits outstanding selectivity against hydrogen, ethanol, and acetone steam. Among them, the sensitivity to ethanol steam is 5 orders of magnitude smaller than that to humidity, while no sensing response is found for hydrogen and acetone. According to the fully recovered performance and non-sensing behavior to hydrogen, the sensing behavior of the nanofibers could be attributed to the electrical-field-driven transfer of proton between H_3O^+ induced by the physisorption of water molecules.

1. Introduction

The monitoring and controlling of the environmental humidity are essential to many applications in fields of industry, agriculture, and biomedicine, etc.[1-4] Therefore, it is of great importance to develop humidity sensors with high sensitivity, fast response, and good repeatability. Up to now, most humidity sensors are either resistance or capacitance type sensors.[4, 5] When the sensing materials absorb water molecules, their impedance or dielectric constant will change.[6] Between the two sensing mechanisms, the resistance type sensors have exhibited many advantages over capacitance type sensors in long-term performance, cost, and processing for mass production.

Recently, semiconductor nanowires have attracted considerable attention as potential highly-sensitive humidity sensing materials. Their high surface to volume ratio and one-dimensional nanostructure may increase their interaction with water molecules. For example, Zhu et al. have fabricated ZnO nanowire-film based humidity sensors, which exhibited high sensitivity and fast response performance. The change of resistance was up to four orders of magnitude to moisture of 97 %RH.[7] Moreover, Si, SnO_2, CuO, TiO_2, CeO_2 and WO_3 nanowires have also been employed as the sensing materials for highly-sensitive humidity sensors.[4, 8-14] However, most semiconductor nanowires are chemically reactive to the oxidizing or reductive gases such as ethanol and acetone steams, as well as NO, H_2, CO, H_2S and NH_4, etc.[15] This deficiency leads to an unstable humidity sensing behaviour in the above mentioned adverse environment. Sodium niobate ($NaNbO_3$) with the perovskite structure has been regarded as a good candidate for lead-containing piezoelectric material with potential applications in energy harvester and pressure sensors, etc.[16, 17] A unique feature of $NaNbO_3$ is its high chemical stability when exposed to environment with chemicals and gases, which inspires us to investigate its potential for stable humidity sensing.

In this work, a humidity sensor based on $NaNbO_3$ nanofiber has been fabricated on interdigitated electrodes by electrospinning process.[18, 19] The sensor exhibits fast response, ultra-high sensitivity and selectivity to the varying humidity. The sensing mechanism of the $NaNbO_3$ nanofiber has also been discussed in detail.

2. Experimental Details

The $NaNbO_3$ nanofibers were directly assembled through a far-field electrospinning process onto a pre-patterned Pt/Ti interdigital electrodes (IDEs) fabricated by a standard lift-off photolithography and sputtering process on a cleaned alumina substrate. The starting precursors for the electrospinning were $NaNbO_3$ sol-gel, poly(vinylpyrrolidone) (PVP) and ethanol. The $NaNbO_3$ sol-gel was prepared using a similar method reported in our previous work,[20] then mixed with the ethanol solution of PVP (MW-1300000, 0.1 g/mL) followed by stirring for 8 h to obtain the $NaNbO_3$ precursor. During the electrospinning process, the $NaNbO_3$ precursor was ejected from the syringe pump at a constant rate of 0.40 mL/h in the electric field of 1.2 kV/cm. After that, the sample was electrospun and collected under low humidity environment, then dried at 80 ^oC for 5 h, followed by a two-step annealing, each for 1 hour, at 450 ^oC and 650 ^oC in the oxygen atmosphere. Finally, a pair of copper leads was glued on the electrodes with conducting silver paste. The phase of the $NaNbO_3$ nanofibers was characterized by X-ray diffractometer (XRD, Bruker D8 Advanced, Cu$K\alpha$, λ = 0.15406 nm). The surface

morphology and composition of the nanofibers were characterized by field emission scanning electron microscopy (FE-SEM, JSM7100F JEOL).

3. Results and Discussions

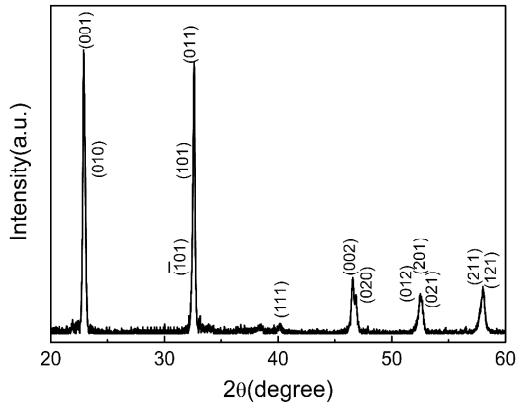

Fig. 1 The XRD pattern of as-synthesized $NaNbO_3$ nanofibers

Fig. 1 shows the XRD pattern of the electrospun samples after annealing at 650 °C in oxygen. The sample is composed of pure perovskite $NaNbO_3$ with monoclinic structure according to the JCPDS card No. 74-2437. The calculated lattice parameters are a = 0.390 nm, b = 0.388 nm and c = 0. 390 nm, β = 90.39°. The average grain size of the $NaNbO_3$ nanofibers is approximately 34 nm according to the Scherrer Equation.

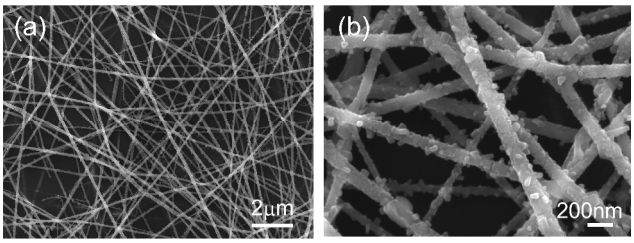

Fig. 2 SEM images of the as-synthesized $NaNbO_3$ nanofibers.

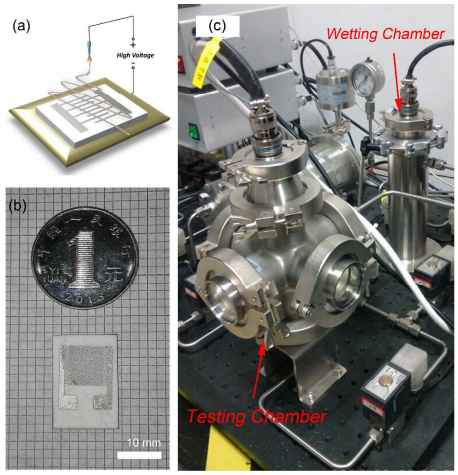

Fig. 3 (a) The schematic illustration of the fabrication process. (b) The photograph of the $NaNbO_3$ nanofiber-based humidity sensor. (c) The performance testing system

Fig. 2 shows the SEM images of $NaNbO_3$ nanofibers fabricated by electrospinning method. As shown in **Fig. 2(a)**, the ultra-long $NaNbO_3$ nanofibers are uniformly distributed on the surface of the substrate. The average diameter of the nanofibers is approximately 100 nm. In addition, there are a large amount of small nanoparticles on the surface of the nanofibers, which can further increase the specific surface area and provide reaction sites during sensing. The EDS result shown in **Fig. S1** confirms that the product is pure $NaNbO_3$ without any other impurities.

IDEs on alumina substrate were employed for building the humidity sensors to increase the defect tolerance induced by the fracture of nanofibers and decrease the resistance of the sensing layers. **Fig. 3(a,b)** show the schematic illustration and photograph of the as-fabricated sensors based on the electrospun $NaNbO_3$ nanofibers. The IDE spacing of the sensor is 200 μm. During the humidity sensing test, the sensors were connected to a Keithley 2400 source meter and positioned into the testing chamber shown in **Fig. 3(c)**. The humidity of the testing chamber was adjusted by introducing either wetting air (through the wetting chamber) or dry air. The relative humidity inside the testing chamber was monitored by a commercial humidity sensor (Honeywell HIH4000).

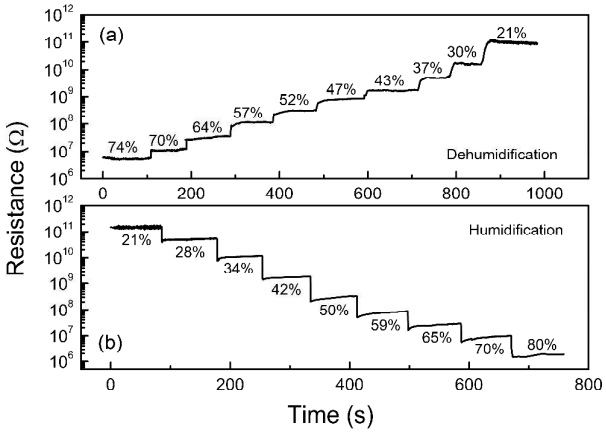

Fig. 4 The electrical resistance variation of the $NaNbO_3$ sensors under different humidity. (a) Dehumidification process, (b) humidification process.

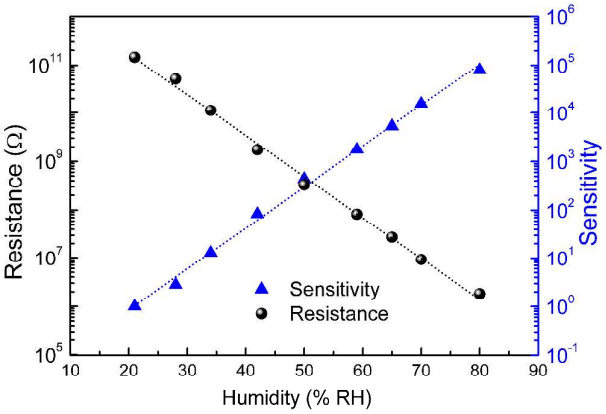

Fig.5 Sensors' resistance (left ordinate) and sensitivity (right ordinate) as a function of the relative humidity.

Fig. 4 shows the variation of sensor's electrical resistance during the step-like dehumidification (a) and humidification (b) processes. As can be seen in **Fig. 4**, the sensor exhibits a responsive step-like change of resistance with respect to the changing humidity and the resistance values are reproducible regardless of dehumidification or humidification process. Moreover, the resistance is changed from ~10^6 Ω at 80 %RH to ~10^{11} Ω at 20 %RH, indicating the ultra-high sensitivity ($S = R_H/R_L \sim 10^5$) of the $NaNbO_3$ humidity sensors (R_H and R_L represent the higher resistance at 20 %RH and lower resistance at 80 %RH humidity respectively). As shown in **Fig. 5,** both the resistance and sensitivity exhibit logarithmic dependence on the relative humidity.

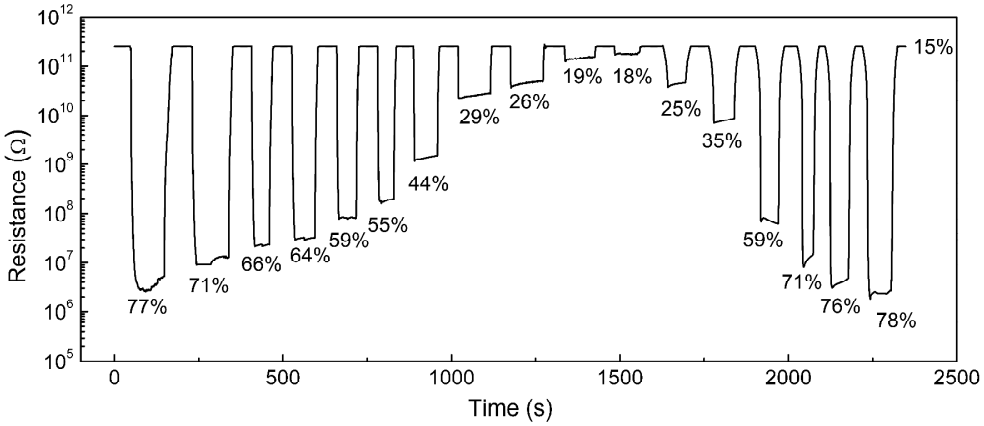

Fig. 6 The variation of resistance during humidification and dehumidification process from 15 %RH to different humidity levels.

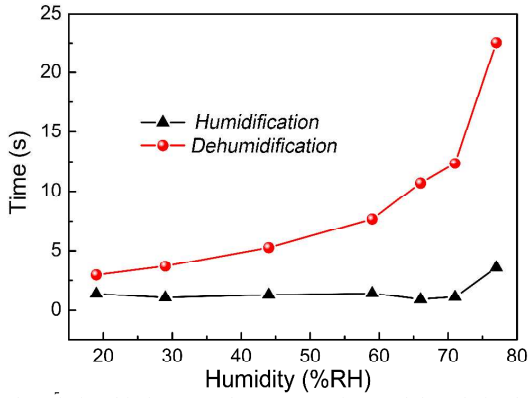

Fig. 7 The relationship between the response time and the relative humidity for the $NaNbO_3$ sensor in humidification and dehumidification process.

In order to estimate the response behaviour to the de-/humidification process, we investigated the variation of resistance with respect to the relative humidity switching from 15 %RH to different values. As can be seen in **Fig. 6**, the resistances have fully recovered to the original value at 15 %RH after each dehumidification cycle, which suggests the high repeatability and stability of $NaNbO_3$ humidity sensors. This result also indicates that physisorption is dominant for the interaction between water molecules and nanofiber surface, because the chemisorption of water molecules on the oxides' surface cannot be completely excluded at room temperature.[10, 21] By defining the response time (t_{res}) as the time to achieve 90 % of the total change, t_{res} for both the de-/humidification processes could be obtained. As shown in **Fig. 7**, this sensor exhibits fast response to the variation of humidity for both processes. Among them, t_{res} for humidification is less than 3 s for all cycles, while that for dehumidification is relatively slower (3 ~ 23 s). Moreover, both response processes become slower when the magnitude of humidity change is increased. The different t_{res} for de-/humidification processes can be attributed to the different rate of absorption and desorption of water molecules by $NaNbO_3$ nanofibers. These differences would be further enhanced at higher humidity levels. Hence, the dehumidification process takes even longer to respond than humidification process does. **Table 1** lists the room-temperature performance of reported resistance-type humidity sensors based on semiconductor one-dimensional nanostructures. The response time of the $NaNbO_3$ nanofibers for both the humidification and dehumidification process is comparable to ZnO nanowires/nanorods, and much shorter than SnO_2 and TiO_2 nanowires.[7,8,10] Moreover, the sensitivity of $NaNbO_3$ nanofibers is much higher than the other kinds of sensing materials. The fast and highly-sensitive humidity sensing performance of the $NaNbO_3$ nanofibers suggests significant potential in humidity detection applications.

Table 1 The room-temperature performance of reported resistance-type humidity sensors based on semiconductor one-dimensional nanostructures.

Materials	Sensitivity	**Response time** (s)		Ref.
		Humidification	Dehumidification	
$NaNbO_3$ Nanofibers	87613	1 - 3	3 - 23	This work
ZnO Nanowires	5443	3	30	[7]
ZnO Nanorods	183	3	20	
SnO_2 Nanowire	33	120 - 170	20 - 60	[8]
TiO_2 Nanowires	~ 10^3	90 - 120	90 - 120	[10]

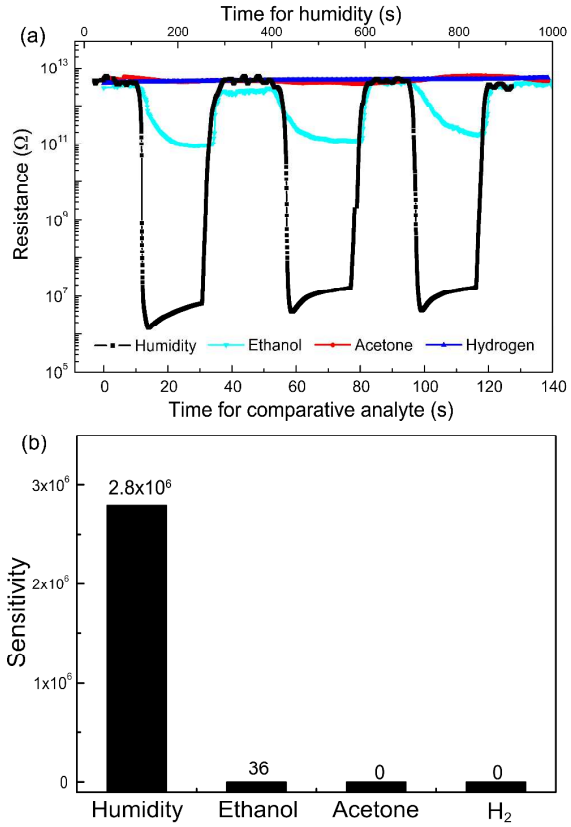

Fig. 8 The selectivity of the $NaNbO_3$ nanofiber-based humidity sensors. (a) The variation of the sensor resistance with exposure to different atmospheres. (b) The sensitivity to different types of gases.

In practical applications, humidity sensors are always exposed to harsh environment composed of complex gas mixtures. Therefore, it is crucial for the sensor to be insensitive to interfering gases especially ethanol, acetone and reducing gases. To investigate the selectivity of the $NaNbO_3$ humidity sensor, we firstly tested its response to high concentration (1 %) hydrogen gas. After that, we replaced the water in the wetting chamber by either ethanol or acetone and used air as the carrier gas to test the sensor response to their steams. During the whole testing processes, the water, ethanol and acetone in the wetting chamber were kept flowing through the inlet bypass to make the concentration in the testing chamber at the same level (high concentration up to 90 %) for all three testing matters. As shown in **Fig. 8(a)**, the $NaNbO_3$ sensor does not show any response to hydrogen and acetone during the three testing cycles, while it exhibits much smaller response to ethanol steam than to humidity. **Fig. 8(b)** shows the sensitivity of the $NaNbO_3$ nanofibers to different gas or steam. The sensitivity to humidity is about 5 orders of magnitude higher than that to ethanol. These results suggest the humidity sensing performance of $NaNbO_3$ nanofibers are not interfered by other types of gases, which is another advantage over humidity sensors based on semiconductor nanostructures.

According to the literature, electrons near the surface of the oxide nanostructures are likely to be trapped by the surface-absorbed oxygen species

$$O_2(g) \leftrightarrow O(ad) \quad (1)$$

$$2O(ad)+e^- \rightarrow O_2^-(ad),\ O(ad)+e^- \rightarrow O^-(ad) \quad (2)$$

An electron depletion layer is then formed on the surface of the $NaNbO_3$ nanofibers, which increases the resistance of the sensing materials due to the small diameter of the nanofibers.[22-24] When the $NaNbO_3$ nanofibers are exposed to wet air, three different reactions may happen on the surface of the depleted nanofibers. Firstly, water molecules may chemisorb on the available sites at the grain boundaries of the polycrystalline nanofibers, and dissociate into hydroxyl (OH^-) and H^+ to form two hydroxyl groups on the surface of the nanofibers. This process can be described as

$$H_2O(g)+Na+O \leftrightarrow (Na^+\text{-}OH^-)+(OH)^++e^- \quad (3)$$

Because electrons are weakly trapped by the proton in the OH^+ group, they are easy to be ionized into free electrons thus leading to increased surface free charge density in the nanofibers.[24, 25] Secondly, other water molecules can be physically adsorbed by hydrogen bonding to the two adjacent chemisorbed OH. Due to the restriction of these two hydrogen bondings, this layer of water molecules is fixed and does not impact the resistance of the nanofibers. However, more water molecules can be absorbed through hydrogen bonding upon the first physisorbed layer.[26] The accumulated water molecule layers decrease the ordering of the molecules near the surface and lead to the dissociation of H_2O into H_3O^+ and OH^-.[27] Although this process may not change the charge carrier density of $NaNbO_3$ nanofibers, the applied electrical field may lead to proton hopping between the neighbouring H_3O^+ groups along the direction of electrical field and increase the conductance of the nanofibers.[21, 28] Thirdly, as reported by Henrich and Cox et al., the pre-adsorbed oxygen species (Equ. 1) can be displaced by the water adsorption at the surface of oxides, which may diminish the depletion layer and increase the free charge carrier density around the surface of the nanofibers.[10, 25, 28] Each of these three mechanisms could contribute to the decrease of resistance near the surface of the nanofibers.

According to the fully recovered sensing performance of the sensors, the change of resistance induced by the chemisorption of OH groups (Equ. 3) is unlikely to be the predominant sensing mechanism as the chemisorbed OH groups cannot be fully eliminated under room-temperature.[10, 21] For the same reason, the third sensing mechanism based on the desorption of oxygen species may not be the main reason for the humidity sensing behaviour of $NaNbO_3$ nanofibers either. As reported, the redox reaction between the pre-adsorbed oxygen species and hydrogen in the atmosphere, which may change the depletion layer, is the major mechanism for the room-temperature hydrogen sensing behaviour of one-dimensional oxide nanostructures.[29, 30] According to **Fig. 8**, the $NaNbO_3$ nanofibers exhibited no response to the hydrogen containing atmosphere during the test. This phenomenon could be attributed to the decreased oxygen vacancy on the nanofiber surface due to the annealing of electrospun nanofibers in an oxygen atmosphere, which is the favourite adsorption site for the oxygen species. As a result, the depletion of electron near the surface (Equ. 1) is suppressed. The poor hydrogen sensing behaviour of $NaNbO_3$ nanofibers also corroborates our finding that the desorption of pre-adsorbed oxygen species cannot be the major sensing mechanism for the humidity sensing behaviour. Therefore, the room-temperature humidity sensing behaviour of the $NaNbO_3$ nanofibers should be attributed to the physisorption of water molecules and the proton hopping among the H_3O^+ groups driven by the applied electrical field. The ultrahigh specific surface area of the $NaNbO_3$ nanofiber networks may enhance this process by providing a large amount of absorption sites for the physisorbed water molecules. Furthermore, the thin diameter of the nanofibers makes surface resistivity predominant in resistivity change of the nanofiber networks, rendering $NaNbO_3$ nanofibers fast and highly sensitive humidity sensing performance.

Conclusions

Ultra-long $NaNbO_3$ nanofibers have been synthesized by the electrospinning process. The as-synthesized nanofibers exhibit monoclinic perovskite structure and high aspect ratio. By connecting them with IDEs, a humidity sensor was successfully developed on alumina substrates. At room temperature, the resistance of the sensors exhibit fast response and high sensitivity to the change of humidity with a logarithmic relationship. The sensitivity is up to 10^5 for the humidity variation from 20 to 80 %RH. Moreover, the response time for the humidification process in all ranges is faster than 3 s, while that for the dehumidification process is relatively slower (3 ~ 23 s). This difference is due to the slower desorption of water molecules than the absorption. In addition, the sensor possesses ultra-high selectivity to water in comparison with ethanol, acetone and hydrogen. It does not respond to hydrogen and acetone steam, and shows 5 orders of magnitude smaller sensitivity to ethanol steam than to humidity. According to the fully recovered humidity response and non-hydrogen sensing behaviour, physisorption of water molecules and subsequent proton hopping between H_3O^+ driven by the applied electrical field are believed to be the dominating mechanism for the humidity sensing.

Acknowledgement

This work was financially supported by the National Science Foundation of China (Grant No. 11474088, 61274073), the National High-Tech Research and Development Program of China (863 Program, Grant No. 2013AA031903) and the Natural Science Foundation of Hubei Province in China (Grant No. 2014CFB557 and 2013CFB038).

Notes and references

[a] Hubei Collaborative Innovation Centre for Advanced Organic Chemical Materials, Faculty of Physics and Electronic Science, Hubei University,

Wuhan, Hubei Province, P.R. China, 430062 E-mail: wangzhao33@hotmail.com

[b] College of Physics, Chongqing University, Chongqing, P.R. China, 400044

[c] Hubei University of Science and Technology, Xian Ning, Hubei Province, P.R. China, 437100.

1. C. Rubinger, H. Calado, R. Rubinger, H. Oliveira and C. Donnici, *Sensors*, 2013, **13**, 2023-2032.
2. Y. Zhen, M. Wang, S. Wang and Q. Xue, *Ceram. Int.*, 2014, **40**, 10263-10267.
3. L. Du, Y. Zhang, Y. Lei and H. Zhao, *Mater. Lett.*, 2014, **129**, 46-49.
4. D. Zhu, Y. Fu, W. Zang, Y. Zhao, L. Xing and X. Xue, *Sens. Actuators, B*, 2014, **205**, 12-19.
5. M. Pandey, P. Mishra, D. Saha, K. Sengupta, K. Jain and S. S. Islam, *J. Sol-Gel Sci. Technol.*, 2013, **68**, 317-323.
6. Z. Ahmad, M. H. Sayyad, M. Saleem, K. S. Karimov and M. Shah, *Physica E*, 2008, **41**, 18-22.
7. Y. Zhang, K. Yu, D. Jiang, Z. Zhu, H. Geng and L. Luo, *Appl. Surf. Sci.*, 2005, **242**, 212-217.
8. Q. Kuang, C. Lao, Z. L. Wang, Z. Xie and L. Zheng, *J. Am. Chem. Soc.*, 2007, **129**, 6070-6071.
9. H. T. Hsueh, T. J. Hsueh, S. J. Chang, F. Y. Hung, T. Y. Tsai, W. Y. Weng, C. L. Hsu and B. T. Dai, *Sens. Actuators, B*, 2011, **156**, 906-911.
10. R.-J. Wu, Y.-L. Sun, C.-C. Lin, H.-W. Chen and M. Chavali, *Sens. Actuators, B*, 2006, **115**, 198-204.
11. C.-L. Dai, M.-C. Liu, F.-S. Chen, C.-C. Wu and M.-W. Chang, *Sens. Actuators, B*, 2007, **123**, 896-901.
12. N. D. Md Sin, M. H. Mamat, M. F. Malek and M. Rusop, *Appl. Nanosci.*, 2013, **4**, 829-838.
13. L. Gu, K. Zheng, Y. Zhou, J. Li, X. Mo, G. R. Patzke and G. Chen, *Sens. Actuators, B*, 2011, **159**, 1-7.
14. J.-L. Hou, C.-H. Wu and T.-J. Hsueh, *Sens. Actuators, B*, 2014, **197**, 137-141.
15. S. M. Kanan, O. M. El-Kadri, I. A. Abu-Yousef and M. C. Kanan, *Sensors*, 2009, **9**, 8158-8196.
16. J. H. Jung, M. Lee, J.-I. Hong, Y. Ding, C.-Y. Chen, L.-J. Chou and Z. L. Wang, *ACS nano*, 2011, **5**, 10041-10046.
17. C. David, J.-F. Capsal, L. Laffont, E. Dantras and C. Lacabanne, *J. Phys. D: Appl. Phys.*, 2012, **45**, 415305.
18. B. Zheng, G. Liu, A. Yao, Y. Xiao, J. Du, Y. Guo, D. Xiao, Q. Hu and M. M. F. Choi, *Sens. Actuators, B*, 2014, **195**, 431-438.
19. Z.-M. Huang, Y. Z. Zhang, M. Kotaki and S. Ramakrishna, *Compos. Sci. Technol.*, 2003, **63**, 2223-2253.
20. D. Zhou, H. Gu, Y. Hu, H. Tian, Z. Wang, Z. Qian and Y. Wang, *J. Appl. Phys.*, 2011, **109**, 114104.
21. S. Jagtap and K. R. Priolkar, *Sens. Actuators, B*, 2013, **183**, 411-418.
22. N. Zhang, Y. Deng, Q. Tai, B. Cheng, L. Zhao, Q. Shen, R. He, L. Hong, W. Liu and S. Guo, *Adv. Mater.*, 2012, **24**, 2756-2760.
23. C. Xiangfeng, L. Xingqin and M. Guangyao, *Sens. Actuators, B*, 1999, **55**, 19-22.
24. Y. Zhao, Y. Ding, X. Chen and W. Yang, *Sens. Actuators, B*, 2014, **203**, 122-129.
25. N. Barsan and U. Weimar, *J. Electroceram.*, 2001, **7**, 143-167.
26. C. O. Park and S. A. Akbar, *J Mater. Sci.*, 2003, **38**, 4611-4637.
27. H. Bi, K. Yin, X. Xie, J. Ji, S. Wan, L. Sun, M. Terrones and M. S. Dresselhaus, *Sci Rep*, 2013, **3**, 2714.
28. S. Liang, X. He, F. Wang, W. Geng, X. Fu, J. Ren and X. Jiang, *Sens. Actuators, B*, 2015, **208**, 363-368.
29. M. Zhao, J. X. Huang and C. W. Ong, *Nanotechnology*, 2012, **23**, 315503.
30. H. Gu, Z. Wang and Y. Hu, *Sensors*, 2012, **12**, 5517-5550.

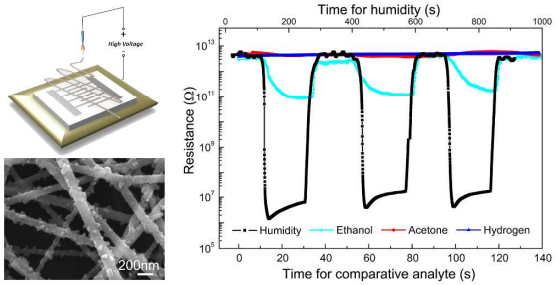

A humidity sensor based on $NaNbO_3$ nanofiber networks with fast, ultra-sensitive and selective room-temperature response was fabricated through electrospinning process.